Neurobiology of Disease 205 (2025) 106793

Contents lists available at ScienceDirect

Neurobiology of Disease

journal homepage: www.elsevier.com/locate/ynbdi

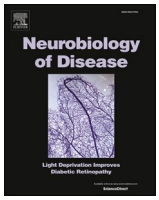

Modeling sacsin depletion in *Danio Rerio* offers new insight on retinal defects in ARSACS

Valentina Naef [a,*,1], Devid Damiani [a,1], Rosario Licitra [a], Maria Marchese [a], Stefania Della Vecchia [a], Matteo Baggiani [a], Letizia Brogi [b], Daniele Galatolo [a], Silvia Landi [c], Filippo Maria Santorelli [a,*]

[a] *Neurobiology and Molecular Medicine Unit, IRCCS Fondazione Stella Maris, 56128 Pisa, Italy*
[b] *Bio@SNS, Department of Neurosciences, Scuola Normale Superiore, 56126 Pisa, Italy*
[c] *Istituto di Neuroscienze-CNR, Pisa, Italy*

ARTICLE INFO

Keywords:
ARSACS
Zebrafish
Retina development
Retinal abnormalities
Neurological disorder

ABSTRACT

Biallelic mutations in the *SACS* gene, encoding sacsin, cause early-onset autosomal recessive spastic ataxia of Charlevoix-Saguenay (ARSACS), a neurodegenerative disease also characterized by unique and poorly understood retinal abnormalities. While two murine models replicate the phenotypic and neuronal features observed in patients, no retinal phenotype has been described so far. In a zebrafish *knock-out* strain that faithfully mirrors the main aspects of ARSACS, we observed impaired visual function due to photoreceptor degeneration, likely caused by cell cycle defects in progenitor cells. RNA-seq analysis in embryos revealed dysfunction in proteins related to fat-soluble vitamins (e.g., TTPA, RDH5, VKORC) and suggested a key role of neuroinflammation in driving the retinal defects. Our findings indicate that studying retinal pathology in ARSACS could be crucial for understanding the impact of sacsin depletion and may offer insights into halting disease progression.

1. Introduction

Autosomal recessive spastic ataxia of Charlevoix-Saguenay (ARSACS) is an early-onset, neurodevelopmental and neurodegenerative condition presenting with ataxia, spasticity and peripheral neuropathy (Bouhlal et al., 2011). Distinctive pathological features include atrophy of the upper cerebellar vermis with loss of Purkinje cells (PCs), corticospinal tract degeneration, axonal damage in both the central and peripheral nervous systems mirrored at the cellular level by aberrant microstructure of neuronal neurofilament network, impaired axonal flow and ensuing disruption of the mitochondrial (Aly et al., 2022; Bagaria et al., 2022; Takiyama, 2006; Vermeer et al., 1993). Clinical and allelic heterogeneity is ample in ARSACS. Although most patients do not show ophthalmological complaints and present normal vision, abnormal thickening of the peripapillary retinal nerve fiber layer (RNFL) observed on optical coherence tomography (OCT) is a distinguishing feature in individuals with ARSACS (Parkinson et al., 2018). OCT, a non-invasive imaging test that uses light waves to take cross-sectional pictures of the retina, revealed in a multicenter study the presence of foveal hypoplasia in nearly all ARSACS cases analyzed, together with a sawtooth retinal appearance with papillomacular folds seen in most cases (Rezende Filho et al., 2021). While in part suggestive of impaired macular function, these findings might represent a long-term complication in ARSACS patients with progressive motor neuron disorder, as well as potential biomarker in future clinical trials. Nonetheless, the natural process of RNFL thickening in ARSACS is unknown, though it is believed to result from the slowing of axoplasmic flow within retinal ganglion cells axons (Borruat et al., 2017). However, there is a phenotypic heterogeneity in patients thickening (Takiyama, 2007; Yu-Wai-Man et al., 2014) and it is of interest that electroretinogram (ERG) data in a patient show inner retinal dysfunction in both rod and cone systems (Borruat et al., 2017), a phenotype that could be explained by the accumulation of proteins at an inner retinal level, or as a secondary effect on retinal bipolar cells (Borruat et al., 2017). Overall, the why and extent of retinal phenotype in ARSACS remain largely unexamined. Building on insights derived from more common genetically-driven retinopathies (Appell et al., 2024), retinal studies might represent a promising target for investigating the consequences of sacsin loss in a controlled niche and an

* Corresponding author.
E-mail addresses: valentina.naef@gmail.com (V. Naef), filippo3364@gmail.com (F.M. Santorelli).
[1] These authors have contributed equally to this work.

https://doi.org/10.1016/j.nbd.2025.106793
Received 8 October 2024; Received in revised form 17 December 2024; Accepted 4 January 2025
Available online 6 January 2025
0969-9961/© 2025 The Authors. Published by Elsevier Inc. This is an open access article under the CC BY-NC-ND license (http://creativecommons.org/licenses/by-nc-nd/4.0/).

attracting system to test efficacy of potential therapies counteracting sacsin depletion. Yet, brain donation programs in neurodegenerative disease face many obstacles and worldwide studies on public attitudes about corneal tissue donation show high rates of unwillingness to donate and donation refusal (Bracher et al., 2021). Thus, it is no surprise that there is limited availability of human tissues in ARSACS (Bagaria et al., 2022). Moreover, no retinal defects have been described to date in the two validated mouse models that phenotypically and neuropathologically replicate sacsin impairment (Larivière et al., 2019; Larivière et al., 2015). With eyes similar to humans in structure and function, zebrafish has become a well-established tool to study vision in vertebrates (Angueyra and Kindt, 2018). Zebrafish are diurnal tetrachromats and have a cone-dominated vision similar to humans, unlike mice presenting a rod-dominated vision due to their nocturnality. Zebrafish retina possesses cone photoreceptors that are sensitive to UV, blue, green, and red light, resulting in excellent color vision and visual acuity (Zang and Neuhauss, 2021). Previously, we modeled sacsin depletion in zebrafish, showing that mutant embryos present with severe motor impairment, hindbrain atrophy recalling PC degeneration, mitochondrial dysfunction, and oxidative stress, mimicking features seen in mice (Naef et al., 2021). In addition, at 48 hpf *sacs*$^{-/-}$ larvae exhibited an increased number of apoptotic cells densely distributed in the ocular area, a finding likely associated with the moderate microphthalmia observed in mutants (Naef et al., 2021). In this work, we further investigated the effects of sacsin loss on retinal development. Our results highlight the critical impact of sacsin on retinal development and visual function. At 120 hpf, the observed disorganization and degeneration of photoreceptors, coupled with the activation of microglia, suggest that neuroinflammation plays a pivotal role in the retinal phenotype of ARSACS.

2. Materials and methods

2.1. Animal experimentation

Adult zebrafish were kept in a recirculating water system at 26 °C–28.5 °C under a 14-h light/10-h dark cycle. Embryos were kept in an E3 medium at 30 °C (Brogi et al., 2021). Zebrafish *sacs* mutants were previously generated as reported in (Naef et al., 2021). All experiments performed in this work comply European Community standards for the use of animals in experimentation under the supervision of the Institutional Animal Care and Use Committee of the University of Pisa, and complied with the 3R principles (MacArthur Clark, 2018).

2.2. Whole mount in situ hybridization

Embryos were dechorionated and fixed at 72 hpf with 4 % Formaldehyde in PBS (FA).Whole-mount in situ hybridization was performed as described previously (Mero et al., 2021).

2.3. Histological analysis and eye morphometry measurement

Larvae were fixed in cold formalin, embedded in agarose blocks, and processed for paraffin embedding. Sections of 5 μm were cut from larval heads and adult eyes, stained with hematoxylin eosin, and examined under a light microscope according to (Sabaliauskas et al., 2006). Images were captured and analyzed using ImageJ software, available from the USA National Institute of Health (http://rsb.info.nih.gov/ij). For eye morphometry measurement, three boxes of 25 × 75 μm were measured for each larva eye.

2.4. Immunofluorescence

To prevent the development of pigmentation, embryos were treated with 0.005 % phenylthiourea from 24 hpf. Whole-mount immunohistochemistry was performed as described in (Della Vecchia et al., 2022). The primary antibody used were: rabbit anti-GFAP (GTX1287, Genetex, 1:200); mouse anti-rhodopsin (ab5417, Abcam, 1:400); mouse anti-Huc/Hud (A21271, Invitrogen, 1:500); rabbit anti-cleaved Caspase 3 (D175, Cell Signalling, 1:200); rabbit anti-PHH3 (phospho-Histone H3, PA5–85506, Invitrogen, 1:500); Rabbit Anti-Zebrafish Blue Opsin Antibody (EJH012, Kerafast, 1:200); Rabbit Anti-Zebrafish UV Opsin Antibody (EJH013, Kerafast, 1:200); mouse anti-acetylated-tubulin (018M4788V, Life Technology, Monza, IT, 1:500); rabbit anti-protein kinase C alpha (PKC alpha, GXGTX130453, Genetex 1:200); the mouse anti-4C4 (1:200) is a gift from Professor Peter Hitchcock, (Department of Ophthalmology and Visual Sciences, University of Michigan, USA).

2.5. Analysis of larvae phenotype

We counted the number of larvae exhibiting thickening of the retinal nerve fiber layer, stained with anti-acetylated tubulin, and calculated the percentage of larvae displaying the phenotype. Out of the 60 larvae analyzed, 20 *sacs* mutant larvae showed thickening of the optic nerve (in both eyes) compared to WT. The analysis performed was qualitative rather than quantitative.

2.6. TUNEL staining

TUNEL staining was performed using the In Situ Cell Death Detection Kit, Fluorescein (11684795910, Roche, Basel, Switzerland) following the manufacturer's instructions as described in (Zhong et al., 2014).

2.7. Quantitative reverse transcription polymerase chain reaction (qRT-PCR)

RNA was extracted from 30 embryos at 120 hours post-fertilization (hpf) using the Quick RNA Miniprep kit (Zymo Research, Irvine, CA) in accordance with the manufacturer's guidelines. cDNA synthesis and qRT-PCR were performed as detailed in a previous study (Naef et al., 2024). Gene expression levels were quantified using the $2^{-\Delta\Delta Ct}$ method (Livak and Schmittgen, 2001). Data from at least three independent experiments were normalized to the expression of the housekeeping gene β-actin (ENSDARG00000037746).

2.8. Electroretinography (ERG)

ERG was performed on zebrafish (both *sacs*$^{-/-}$and controls) at 5 dpf. Each individual larva was anaesthetized with tricaine and stimulated with flashes of 7 different light intensities with an interval of 60 s between each flash, given by high power led light source with liquid light guide hpx-l5 (Sutter Instruments, Novato, CA). The recording settings were performed as already described and readapted (Masek et al., 2023), electrophysiological signals were amplified 1000-fold (EXT-02F, NPI,Tamm, Germany), band pass filtered (0.001–0.3 kHz), and digitized at a rate of 10 kHz (Axon Digidata 1550B, Clampex 10.7.0.3, Molecular Devices, Berkeley, CA) and flash luminance was detected in cd*s/m2 by using a photometer (Konica Minolta) and represented as a logarhythm. The corresponding ERG b-wave amplitude was quantified as already described (Marchese et al., 2024).

2.9. Optokinetic response (OKR)

The optokinetic response of zebrafish larvae was evaluated to identify visual system defects according to (Camussi et al., 2024). Larvae were immobilized in 5 % methyl cellulose on an inverted Petri dish and placed in the VisioBox (ViewPoint Behavior Technology, Lyon, France), where black and white vertical stripes were projected. Eye movements (saccades) were measured using PHIVisualize software, with results expressed as saccades per minute.

2.10. Visual background adaptation (VBA) reflex

Larvae at 120 were placed in petri dishes and immobilized in 1 % agarose low melting for 20 min of darkness, followed by immediate dorsal view imaging. After this, the larvae were exposed to bright light for 15 min, and images were taken in the same way according to (Le et al., 2012).

2.11. Locomotor behavior

The visual motor response test (VMR) was conducted on hatched larvae at 120hpf, using 96-well plates (1 larva/well) positioned in the DanioVision system connected with EthoVision XT17 software (Noldus Information Technology). Following acclimatization to the recording chamber, zebrafish were adapted to stable lighting conditions (450 mW/m^2) for 30 min, after which illumination was abruptly discontinued (lights ON vs. lights OFF) according to (Maurer et al., 2010). Light/dark background preference test was performed according to (Steenbergen et al., 2011; Rock et al., 2022).

2.12. RNA-sequencing

Total RNA was extracted from 30 zebrafish larvae at 120 hpf for each sample using the Quick RNA miniprep kit (ZymoResearch, Irvine, CA, USA), according to the manufacturer's instructions, and checked for purity using NanoPhotometerTM Pearl, version 1.2 (IMPLEN, Westlake Village, CA, USA). Three biological replicates were used for each analyzed condition (*sacs*$^{-/-}$ and controls larvae). Libraries were prepared with from 350 ng of total RNA using the TruSeq Stranded kit (Illumina, San Diego, CA, USA), quantified by real-time PCR, pooled at equimolar concentration, and sequenced with Illumina technology applying standard manufacturer protocols. Reads were aligned to the zebrafish reference genome assembly (GRCz11) using the STAR aligner (http://code.google.com/p/rna-star). To allow comparison of gene expression profiles, the normalized gene abundance level of the controls was compared with the profile of *sacs*$^{-/-}$ and reported as log2 fold change (log2(FC)). Transcripts showing a log2(FC) $\geq$ 0.58 and an adjusted *p*-value (p-adj) $\leq$ 0.05 were considered differentially expressed. GO chord plots were plotted by using a free online platform for data analysis and visualization: https://www.bioinformatics.com.cn/en.

2.13. Protein-protein interaction network construction and module analysis

Protein-protein interaction (PPI) information was obtained through an online STRING analysis (https://string-db.org/). Proteins were clustered using the "K-Means" clustering algorithm. The" K-Means" algorithm finds a defined number of clusters based on their centroids. The clusters were identified based on the Cellular Components and Biological Process.

2.14. Quantification of microglia morphology

Roundness index is defined as 4 × Area/ (π × Major Axis2), with values ranging from 0 (indicative of a linear shape) to 1 (indicating a perfect circle). A value of 1 indicating an amoeboid shape and a value of 0 indicating a highly ramified morphology. Microglial roundness was quantitatively assessed using ImageJ software (https://imagej.net/ij/; National Institutes of Health, Bethesda, MD, USA). Images of microglia were first converted to grayscale by selecting Image > Type > 8-bit. To enhance the visibility of the microglial cells, a threshold was applied (Image > Adjust > Threshold), adjusting the sliders until the cells were highlighted in red. The images were then converted to binary format (Process > Binary > Make Binary), where the microglia appeared as white objects on a black background. In cases where cells were clumped together, the Watershed function (Process > Binary > Watershed) was used to separate them. Particle analysis was performed (Analyze > Analyze Particles) with size parameters set to exclude noise, ensuring only the cells of interest were measured.

2.15. Statistical analyses

All data in the manuscript represent three or more independent experiments giving similar results. We performed the statistical analysis using GraphPad Prism 6 software. All data were analyzed using either parametric or non-parametric methods, based on the distribution of the response variable as determined by the Shapiro–Wilks test. Homogeneity of variance was checked with the Levene test. The significance between groups was determined using two-way Anova Bonferroni's multiple comparisons test or the Kruskal Wallis test or the non-parametric two-tailed Mann-Whitney rank sum test, as indicated in each figure legend. Statistical analysis for qRT-PCR experiments was performed using the two-tailed paired Student's *t*-test. Statistical significance is reported as: * $p < 0.05$, ** $p < 0.01$, *** $p < 0.001$, or **** $p < 0.0001$.

3. Results

3.1. Zebrafish *sacs*$^{-/-}$ mutants showed normal eye morphology but affected lamination of the retinal layers

Previous studies in zebrafish have described mRNA *sacs* expression patterns in the early embryos (24 hpf) (Romano et al., 2013) but no data on later stages are available in the literature. To fill this gap, we performed whole mount in situ hybridization (WISH) at 72 hpf, a critical stage for retinal development, revealing that *sacs* mRNA is localized in the most anterior region of the central nervous system and in the eye fields (Fig. 1A), specifically in the periphery of the retina (Fig. 1A'). To investigate putative mechanisms of moderate microphthalmia (Naef et al., 2021) in *sacs*$^{-/-}$ mutant larvae, we examined their retinal morphology through hematoxylin/eosin staining of retinal sections of 120 hpf larvae. The results showed that there was no obvious difference in cell layer organization between mutant and controls (Fig. 1B). On the other hand, we observed significantly reduced thickness of retinal pigmented epithelium (RPE) (25 %), Outer Nuclear Layer (ONL) (11 %), Inner Nuclear Layer (INL) (30 %), and Ganglion Cellular Layer (GCL) (37.5 %) compared to control embryos (Fig. 1B'). In addition to defects in retinal layer formation, *sacs*$^{-/-}$ mutants presented expanded pigmentation in skin melanocytes even when exposed to bright light for 15 min (Fig. 1C). This phenomenon is indicative of an impaired visual background adaptation (VBA) reflex and suggestive of altered visual responsiveness (Letelier et al., 2023).

3.2. Visual behavior is impaired in zebrafish mutants

To quantitatively characterize eye performance, optokinetic response (OKR) recordings were obtained for control and *sacs*$^{-/-}$ larvae, following an established protocol (Rodwell et al., 2023). We observed that 120 hpf *sacs*$^{-/-}$ mutants showed a significant reduction in the frequency of saccades, with an average of 12 saccades per minute compared to 15 saccades recorded in controls (Fig. 2A). These results confirmed that *sacs*$^{-/-}$ mutants exhibit deficits in visual function. Then, we performed light/dark background preference behavior (Chen et al., 2018) in a 24-well plate apparatus prepared to achieve equal light and dark areas (Fig. 2B). Notably, *sacs*$^{-/-}$ mutants exhibited freezing behavior in the light condition (crossed time/min) and did not show a preference for the bright/white (% time in the light area) area during the dark phase when compared to controls (Fig. 2B). We also tested our *sacs*$^{-/-}$ mutants using the visual-motor response (VMR) assay, useful for measuring the responsiveness of zebrafish larvae to light changes (Venkatraman et al., 2020). At 120 hpf zebrafish *sacs*$^{-/-}$ larvae showed an affected VMR (Fig. 2C), as their motor activity appeared significantly higher in the

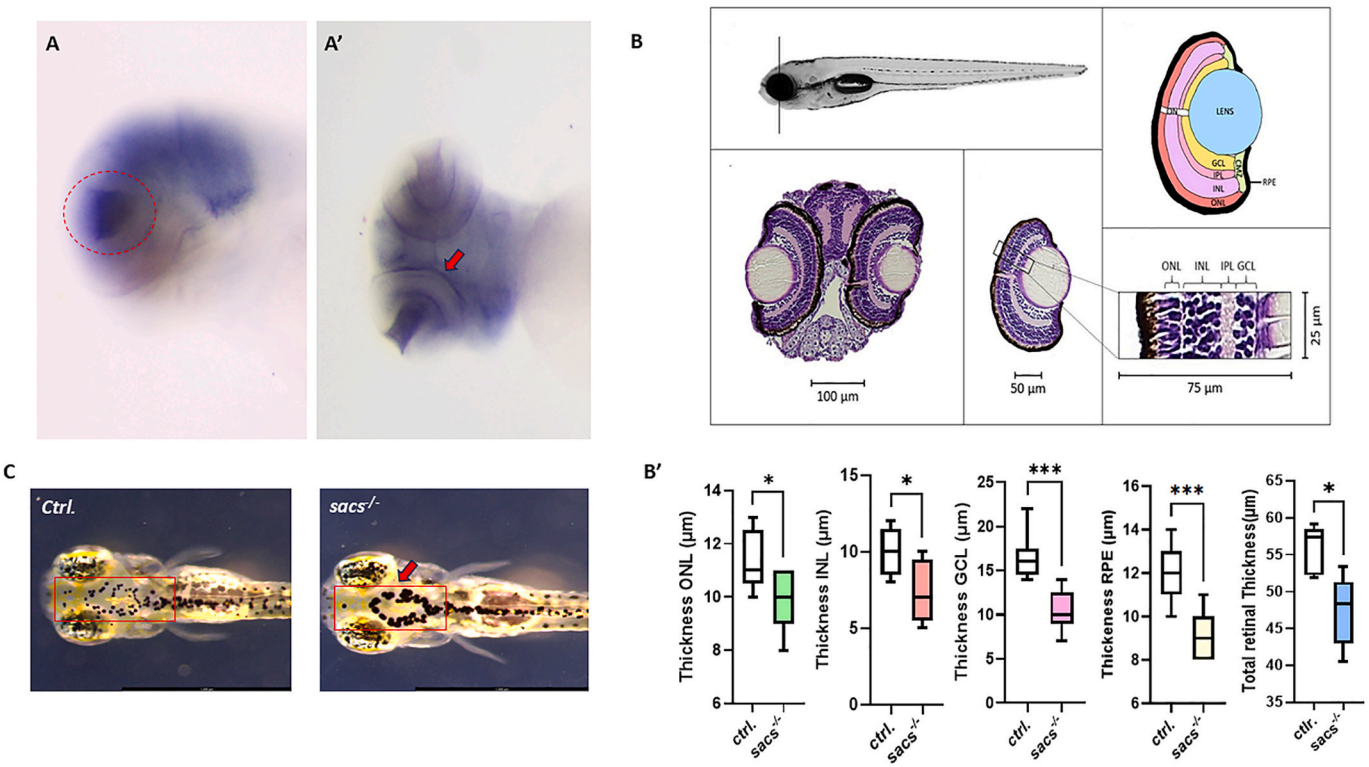

Fig. 1. Loss of *sacs* gene affect neural retina formation and altered VBA reflex. (A) At 72 hpf *sacs* gene is expressed in the most anterior region of the CNS and in the eye field (red circle in A, lateral view; red arrow in A', ventral view). (B-B′) Hematoxylin/eosin staining revealed a normal organization in retina structure in *sacs*$^{-/-}$ larvae and reduced thickness of ONL (the outer nuclear layer), INL (inner nuclear layer), GCL (ganglion cell layer), and in RPE (retinal pigmented epithelium) and in total retinal thickness. Error bars indicate mean ± s.e.m. Statistical differences were computed using the two-tailed Mann-Whitney test and are indicated as (*$p <$ 0.05; ***$p < 0.001$). (IPL (inner plexiform layer)). Results were obtained from representative sections from 5 zebrafish control embryos and 5 *sacs*$^{-/-}$ mutant larvae. C) Head dorsal view of 120 hpf control and *sacs*$^{-/-}$ larvae with insets showing their pigmentation pattern (red arrow). Scale bar = 100 µm. (For interpretation of the references to colour in this figure legend, the reader is referred to the web version of this article.)

"light-OFF" condition compared to control siblings, and greatly reduced in the "light-ON" condition (Fig. 2C'). Even if at the dark-light transition a synchronous and abrupt decrease in motor activity was observed in both control and *sacs*$^{-/-}$ larvae, a finding corresponding to the O-bend response (Burton et al., 2017), we observed that larval motor activity of mutants remained strongly decreased compared to control larvae (Fig. 2C).

3.3. Zebrafish mutants showed failure in the balance between proliferation and differentiation

As we observed alterations in the thickness of retinal layers, we examined sacsin-deficient retinas for potential cell cycle defects and/or cell death imbalances. In zebrafish, a single pool of multipotent progenitors undergoes symmetric proliferative divisions to expand the tissue and gives rise to all retinal cell types (Wan and Goldman, 2016). To investigate proliferation defects, we immunolabeled control and *sacs*$^{-/-}$ mutants for the M-phase nuclear marker phosphohistone-H3 (PHH3). Despite the high proliferative rate of the eye primordium at 24–30 hpf (Letelier et al., 2023), confocal imaging revealed a significant increase in M-phase positive nuclei in *sacs*$^{-/-}$ compared to control eyes (Fig. 3A). In addition, although the proliferation wave has largely completed in control eyes by 60 hpf (Letelier et al., 2023), retinal progenitors in 120 hpf mutant fish continued to divide, as evidenced by a significant increase in PHH3+ cells, particularly in the outer and peripheral regions (Fig. 3B). These findings suggest that loss of sacsin might lead to an extended period in which retinal progenitor cells (RPCs) remain cycling, resulting in a consequent delay in cell cycle exit. The increase in M-phase positive nuclei was also observed in other brain regions (yellow and blue arrows Fig. 3C), such as the optic tectum and the eye, and accompanied by defects in axonal outgrowth as shown by immunofluorescence for acetylated-α tubulin, labeling post-mitotic neurons (Fig. 3D). Additionally, one-third of *sacs* mutants larvae compared to WT stained with acetylated-α tubulin showed thickening of the optic nerve in both eyes (yellow arrow, Fig. 3E-E'). This low penetrance of the phenotype could be explained by the fact that abnormal retinal thickening is a common, although not universal, feature among patients with ARSACS (Yu-Wai-Man et al., 2014). An increase in cell proliferation typically leads to an imbalance in the timing of differentiation, resulting in a reduction of early-born retinal neurons, such as retinal ganglion cells (RGCs), in favor of later cell types, including amacrine, bipolar, and Müller glial cells (Miles and Tropepe, 2016). Given the observed microphthalmic phenotype in larvae and the unexpected reduction in cellular counts in the inner nuclear layer (INL), we investigated potential modifiers of the underlying pathological mechanisms beyond unbalanced neurogenesis. Since apoptosis might contribute to this condition (Miles and Tropepe, 2016), we assessed whether retinal cells undergo apoptosis. We performed a TUNEL assay (Fig. 4A-A') and stained retinal cryosections at 120 hpf with anti-cleaved caspase-3 (C3) antibodies (Fig. 4B-B'). While control retinas exhibited few fluorescent apoptotic TUNEL+ cells (Fig. 4A-A'), a significant increase in apoptotic cells was observed in the sacs-deficient larvae. Consistently, *sacs*$^{-/-}$mutants showed a significant increase in the number of apoptotic C3+ cells compared to controls (Fig. 4A-A'). Apoptotic cells were mainly observed in the INL, suggesting that cell death in this layer may contribute to the decreased thickness observed in *sacs*$^{-/-}$ retinas. Additionally, we observed apoptotic cells in the GCL and the ONL in *sacs*$^{-/-}$ mutants, indicating compromised survival of these cells. These findings suggest that increased apoptosis in neural retina cells may underlie the microphthalmia phenotype and potentially contribute to impaired vision.

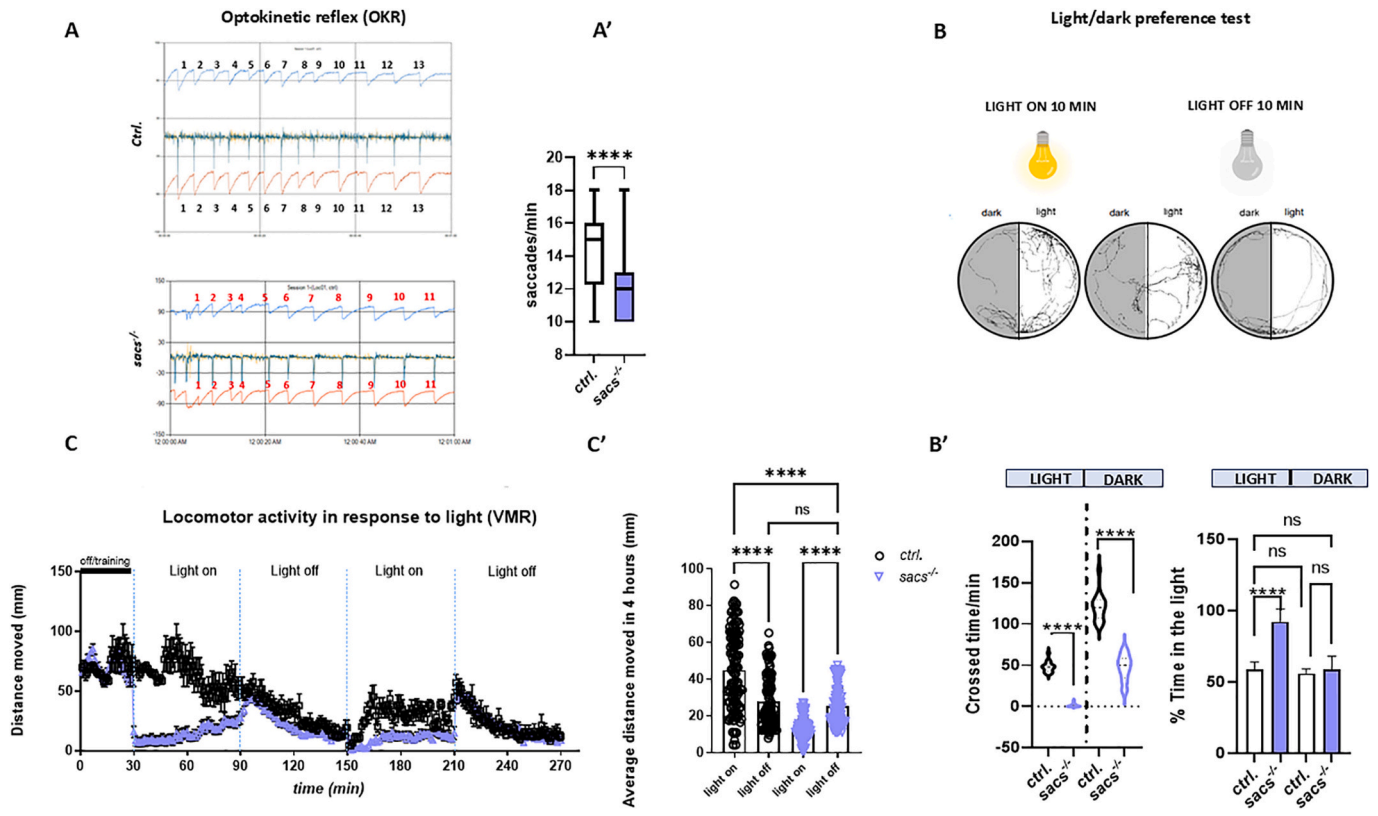

Fig. 2. Visual impairment in the *sacs*$^{-/-}$ larval zebrafish. (A-A') Zebrafish *sacs*$^{-/-}$ mutant larvae at 120 hpf showed reduced optokinetic response. The frequency was calculated considering the number of saccades per minute for each larva examined ($N = 40$ for each group, *sacs*$^{-/-}$ and controls). (B-B′) Light-Dark preference test was performed according to (Rock et al., 2022). At 120 h post-fertilization, *sacs*$^{-/-}$ mutant larvae displayed freezing behavior under light conditions (measured as crossed time per minute) and showed no preference for the bright/white area during the dark phase (measured as percentage of time spent in the light area ($N = 15$ for each group,*sacs*$^{-/-}$and controls). ****$p < 0.0001$ was calculated by Kruskal Wallis test multiple comparisons. (C-C′) Zebrafish *sacs*$^{-/-}$ mutant larvae at 120 hpf showed an affected visual motor response (VMR). *Sacs*$^{-/-}$ mutants motor activity appears significantly higher in light- off conditions compared to controls siblings and greatly reduced in light-on condition ($n = 20$ for each group, *sacs*$^{-/-}$ and controls). ****p < 0.0001 was calculated by two-tailed Mann-Whitney test. Error bars indicate mean ± s.e.m.

3.4. Loss of sacsin leads to structural disorganization and loss of photoreceptors in the ONL

The results so far indicate that sacsin is not essential for the early specification of the neural retina in zebrafish. This finding allowed for a detailed analysis of cell fate choices in *sacs* knock-out larvae. Although all retinal layers are present, the specific identities of the cells within these layers required further investigation. Analysis at 120 hpf revealed no significant decrease in bipolar cells (white arrows, Fig. 5A'), but an increase in HuC-positive cells, a marker for differentiated amacrine cells, was evident by evaluation of mean fluorescence intensity (Fig. 5B) suggesting that loss of sacsin may play a crucial role in regulating amacrine cell specification (white arrows, Fig. 5B'). Additionally, we stained larvae for markers off terminal differentiation in rods (anti-rhodopsin) and cones (blue-opn1sw and uv-opn1sw) at 120 hpf (Fig. 5C-E'). Analysis of rhodopsin mean fluorescence intensity revealed significant increase in knockout larvae (Fig. 5C). High magnification confocal microscopy determined that most of the signal was concentrated in photoreceptor outer segments, with clear alterations in the structure and morphology of both rod and cone photoreceptors in mutant larvae (white arrows, Fig. 5D'-F'). These findings support the hypothesis that sacsin ablation causes retinal dysplasia, particularly affecting the fine morphology of photoreceptor cellular structure.

3.5. Mutants exhibited an increase in b-wave amplitude after light stimulation

To better characterize the different response to the light/dark stimulus of *sacs*$^{-/-}$ mutant larvae, we performed ERG recordings at 120 hpf (Fig. 6A-B), a time point in development when zebrafish retina becomes fully functional, with the exception of late-maturing rods; at this stage the recorded field potentials were mainly contributed by cones. In our hands, control larvae showed a standard ERG response to light flashes, characterized by a large positive b-wave representing the depolarization of ON bipolar cells, which also masks the initial a-wave generated by photoreceptor (PR) hyperpolarization. We found that b-wave amplitude in *sacs*$^{-/-}$mutant larvae appeared to be increased in most light conditions compared to their counterparts (Fig. 6A-B). The b-wave reflects ON-pathway activation and can serve as a proxy for the general excitability of the outer retina. These results demonstrate that there is no adverse effect on outer retina function, but the significant increase of the b-wave amplitude in the ERG of *sacs*$^{-/-}$ mutants suggests higher light sensitivity in mutants if compared to controls. This could be due to putative alterations in retinal dopamine and ON-pathway activity, which may enhance the photopic cone response by reducing negative feedback from horizontal cells in *sacs*$^{-/-}$ mutant retinas (Niklaus et al., 2017).

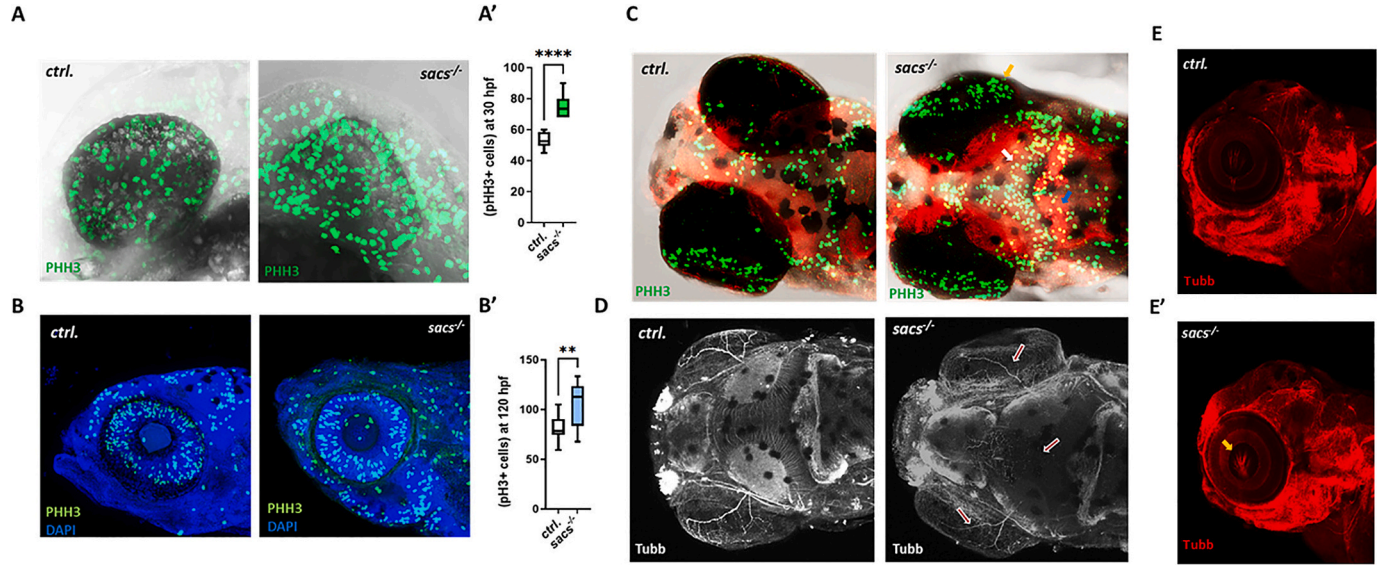

Fig. 3. Zebrafish mutants lacking the *sacs* gene exhibited an imbalance between cell proliferation and differentiation. (A-B). Representative figure of anti-pH 3 immunostaining. A-A') Lateral view pictures of control and *sacs*$^{-/-}$ specimens. At 24 hpf homozygous larvae showed a significant increase in pH 3-positive cells that were counted in the whole eye area. **** $p < 0.0001$ was calculated by the two-tailed Mann-Whitney *U* Test. Error bars indicate mean ± s.e.m. (B-B′) Anti-pH 3 immunostaining at 120 hpf in controls and *sacs*$^{-/-}$ mutant larvae. ** $p < 0.01$, Statistics were calculated by two-tailed Mann-Whitney U Test. (C) Representative fluorescence images of anti-pH 3 immunostaining at 120 hpf (dorsal view) in controls and *sacs*$^{-/-}$ mutant larvae. (D) Immunostaining of acetylated-α tubulin. Dorsal view pictures of representative control and *sacs*$^{-/-}$specimens. Red arrows indicate defects in axonal outgrowth. (E) Representative immunostaining of acetylated-α tubulin at 120 hpf (lateral view). *sacs*$^{-/-}$ *mutants* exhibited alteration in optic nerve thickness (yellow arrow). All images were acquired using a Zeiss LSM 900 confocal-microscope. PHH3+ cells were counted per area. Scale bar = 50 μm (A) and 10 μm (B). (For interpretation of the references to colour in this figure legend, the reader is referred to the web version of this article.)

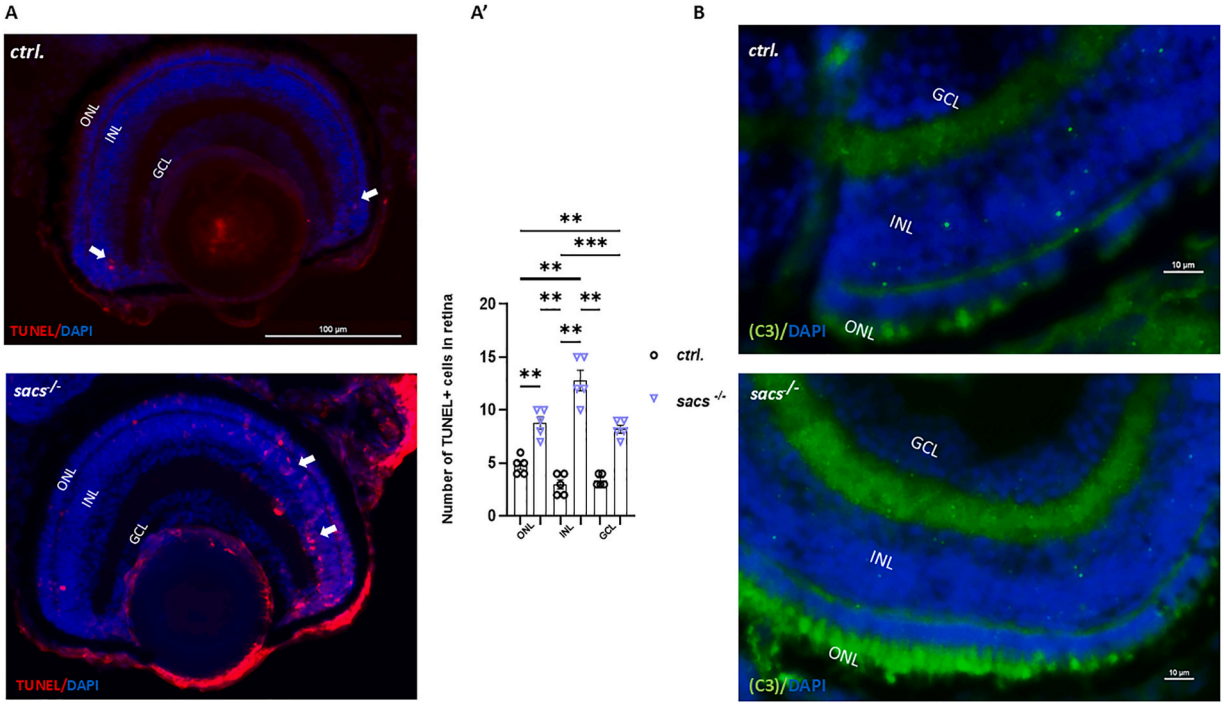

Fig. 4. Increased apoptosis contributes to retinal defects in *sacs*$^{-/-}$ zebrafish mutants. (A) Representative TUNEL staining on retinal frozen section of zebrafish larvae at 120 hpf from control embryos and mutants. (A') Quantification of the number of TUNEL-positive cells in the entire retina based on three independent measurements of larvae per group at 120 hpf. ** $p < 0.01$; *** $p < 0.001$ were calculated by Kruskal Wallis test multiple comparisons. (B) Immunostaining of the retinal section with activated Caspase-3 antibody (green) at 120 hpf. Nuclei were highlighted with DAPI (blue). ONL, outer nuclear layer; INL, inner nuclear layer, GCL, ganglion cell layer. Scale bar = 100 μm (A) and 10 μm (B). All images were acquired using a Zeiss LSM 900 confocal-microscope. TUNEL+ cells were counted per area considering whole retina section. (For interpretation of the references to colour in this figure legend, the reader is referred to the web version of this article.)

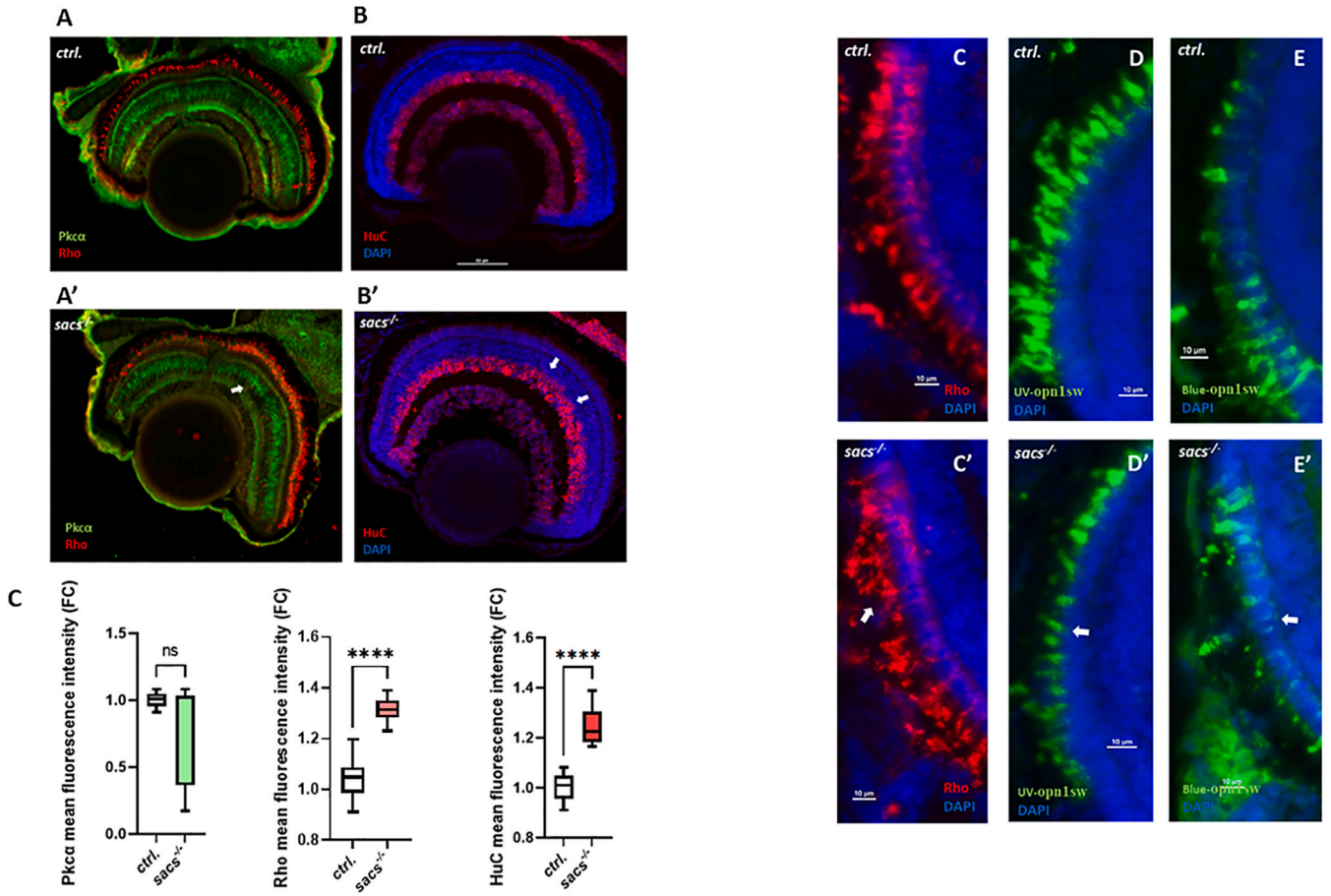

Fig. 5. Sacsin deficiency alters cell fate and photoreceptor structure in zebrafish retina (A) Representative confocal images of the retina of *sacs*$^{-/-}$ zebrafish obtained after immunostaining of rods with a rhodopsin antibody (red) and with PKC-α to label bipolar cells. (B) Immunostaining of amacrine cells with a HuC antibody (red). Nuclei were highlighted with DAPI·(C) Analysis of fluorescence mean intensity in knockout larvae compared to controls. (D-F′) Representative confocal images of the retina of *sacs*$^{-/-}$ zebrafish obtained after immunostaining of rods with a rhodopsin antibody (red) and cones (Uv-opn1sw and Blue-opn1sw) in green. Scale bar = 50 μm (A-B′) and 10 μm (C-D′). (For interpretation of the references to colour in this figure legend, the reader is referred to the web version of this article.)

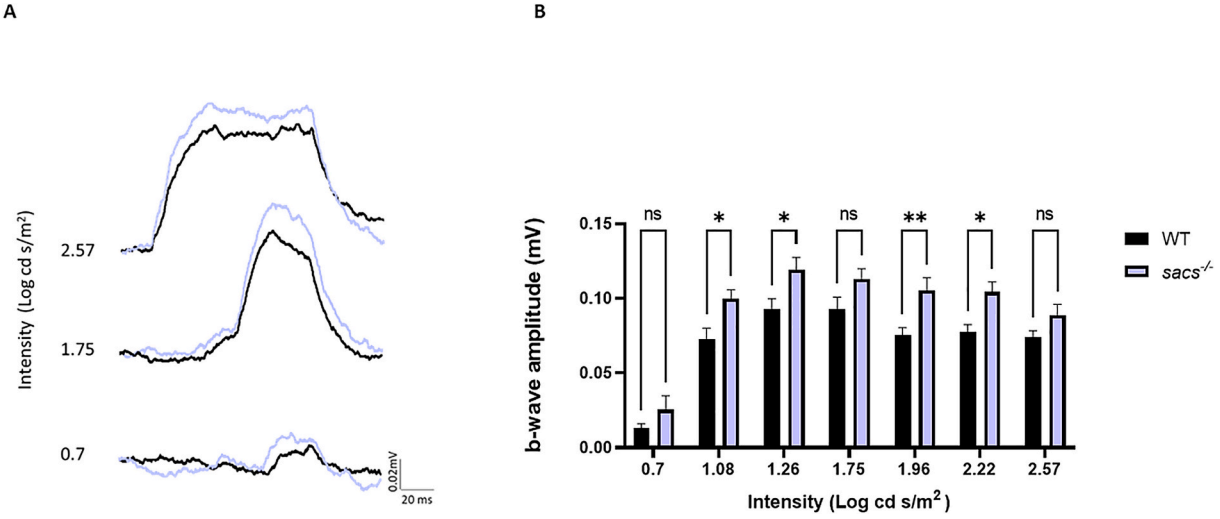

Fig. 6. ERG response is increased in *sacs*$^{-/-}$ larvae. (A) Representative ERG traces at low, medium and maximum light intensity from control (black), *sacs*$^{-/-}$ (blue) at 120 hpf. (B) Averaged ERG b-wave amplitudes from control (black), *sacs*$^{-/-}$ (blue) larvae. *Sacs*$^{-/-}$ mutants produce an increase of the ERG b-wave amplitude compared with control throughout all light intensities tested (*p < 0.05, **p < 0.01). Data were collected from three independent experiments ($N = 30$ for each group, *sacs*$^{-/-}$ and controls). For statistical comparison, a two-way ANOVA test was used. (ns: not significant; SI unit for luminance is candela per square meter (cd/m^2)). (For interpretation of the references to colour in this figure legend, the reader is referred to the web version of this article.)

3.6. RNA-seq analysis revealed changes in mitochondrial pathways and an impairment in fat-soluble vitamins

To characterize the effects of the loss of sacsin during zebrafish development, we performed RNA-seq comparing three different pools of *sacs*$^{-/-}$ mutants and control whole larvae at 120 hpf. The transcriptomic profiles identified 488 differentially expressed gene transcripts (DEGs) in *sacs* null-embryos, of which 269 were up-regulated and 219 down-regulated (Supplementary file) (see also Fig. 7A). By gene ontology (GO) analysis we found an impairment in the fat-soluble vitamin-related protein TTPA (alpha-tocopherol transfer protein) and other proteins involved in vitamin metabolism and mitochondrial function (Fig. 7A-B). These results are particularly intriguing given that chronic deficiency or dysregulation of vitamin E can result in irreversible damage to the nervous system due to the accumulation of oxidative damage (Olufunmilayo et al., 2023) and could be associated with the development of eye disorders (Davison, 2020). Notably, among other DEGs in mutant larvae we identified the downregulated retinol dehydrogenase 5 (*rdh5*) gene. This gene plays a significant role in the retinoid cycle metabolic pathway, also known as the visual cycle. The visual system produces the visual chromophore, 11-cis-retinal, from dietary vitamin A, all-trans-retinol, making this vitamin essential for retinal health and function (Sahu and Maeda, 2016). Transcriptomic data validation was carried out through real-time PCR on multiple genes found to be differentially expressed (Fig. 7C). Furthermore, using STRING (https://string-db.org/), we performed a Protein-Protein Interaction Analysis (PPI) that revealed multiple up-regulated proteins related to the inflammatory response and oxidative stress in *sacs*$^{-/-}$ mutants compared to controls (Supplementary Fig. 1) and down-regulated proteins related to mitochondrial activity and oxidative phosphorylation (Supplementary Fig. 2).

3.7. Mutant retinas displayed activation of Müller Glia and inflammatory response

A chronic inflammatory response in the zebrafish retina can cause tissue damage, worsen neurodegeneration, and hinder the retina's natural regenerative abilities (Iribarne and Hyde, 2022). Clearance of apoptotic cells in the developing retina occurs by microglia during normal retina development, and recent experimental work supports a role for inflammation and resident microglia in the regeneration of rod photoreceptors in zebrafish (Mitchell et al., 2018). Under normal conditions, retinal microglia morphology is ramified with long processes and integrated among the highly organized retinal tissue. Generally, when responding to neurological insults, microglia transform morphology from ramified to an ameboid shape and migrate to sites of cell death (Guo et al., 2022). Based on this background, using the 4c4 antibody that recognizes lgals3bpb, a predicted highly glycosylated protein functioning in the microglial lineage (Rovira et al., 2023), we found activated microglia that appeared ameboid in shape and largely localized in the GLC and the outer mutant retina (Fig. 8A-E). Hyperactivation of microglia/macrophages could induce chronic inflammation, thereby forming a positive feedback loop (Shao et al., 2022) that is both detrimental to the injured tissue and could be incompatible with regeneration. Additionally, inflammation can impair the regenerative functions of Müller glia, which are crucial for retinal repair and regeneration (Koke et al., 2010). In a healthy retina, Müller glia are located in the INL in a quiescent state and function by providing structural and functional support to the retinal neurons (Koke et al., 2010). Following retinal damage, in response to pro-inflammatory molecules released by

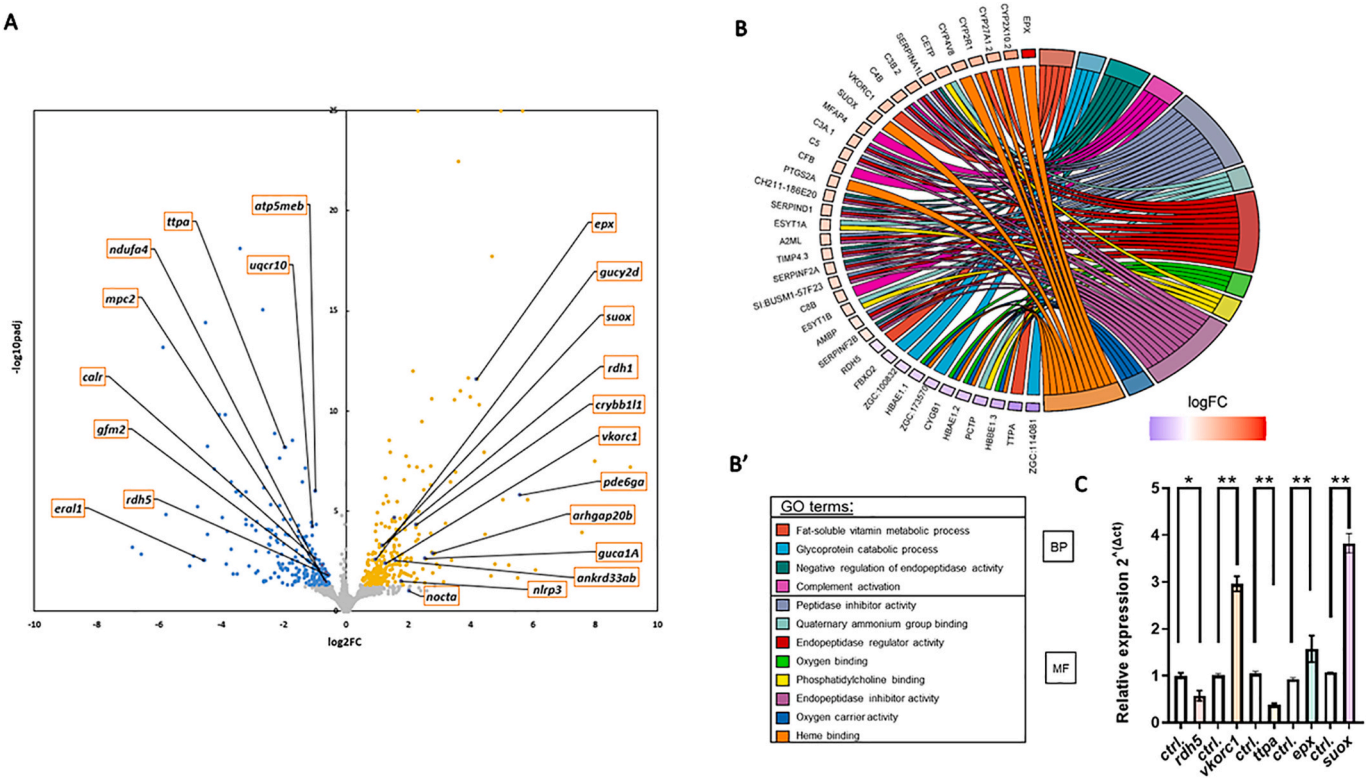

Fig. 7. RNA-seq analysis revealed mitochondrial pathway changes and fat-soluble vitamin deficiency. (A) Significant genes with padj<0.05 and log2FC > 0.58 or log2FC < −0.58 are highlighted in yellow or blue, respectively. Genes not significantly expressed are represented by grey points. (B) The top enriched Biological Processes GO categories have then been plotted. Loss of sacsin during early development leads to an impairment in fat-soluble vitamin related protein (e.g TTPA) and other proteins involved in mitochondrial function and metabolism. Relative mRNA expression of DEGs genes were evaluated in *sacs*$^{-/-}$ larvae at 120 hpf normalized to β-actin. Three independent RNA samples from *sacs*$^{-/-}$ mutant larvae at 120 hpf and from controls. *p < 0.05 or **p < 0.01 were calculated by two-tailed Student's *t*-test. Error bars indicate mean ± s.e.m. (For interpretation of the references to colour in this figure legend, the reader is referred to the web version of this article.)

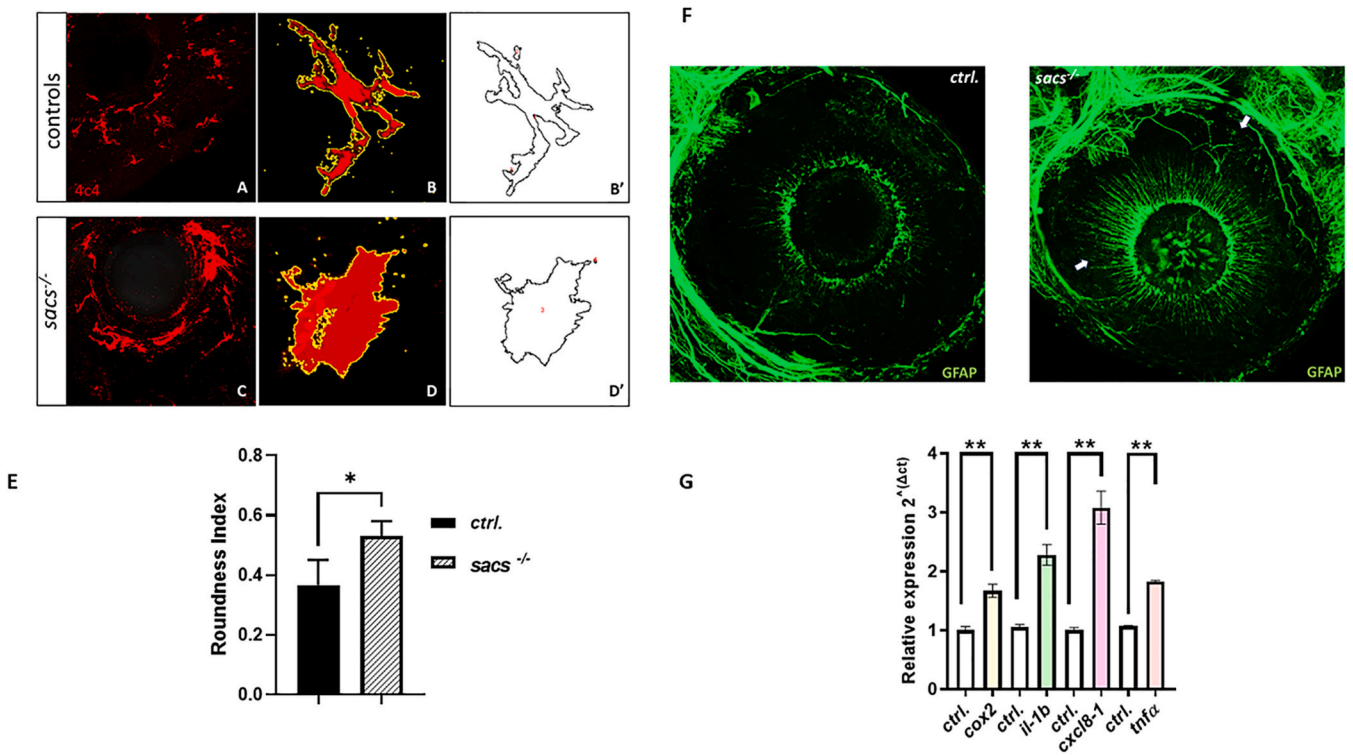

Fig. 8. *sacs*$^{-/-}$ mutant retinas showed Müller glia activation and inflammation (A and C) Eye confocal images of control and *sacs*$^{-/-}$ larvae obtained after immunostaining with antibody 4C4, which is specific for zebrafish microglia. (B and D) cell digital image. After random selection of cells from the eye picture (A and C), the noise was removed by filtering the overall background to get a shape extraction. Next, the image was changed to grayscale, and then transformed into a binary image. The binary image was edited to clear the background and to join all branches (B′ and D′). (E) Quantification of the roundness index revealed activated microglia in *sacs*$^{-/-}$ larvae which appeared ameboid in shape. *$p < 0.05$ was calculated by two-tailed Mann-Whitney U Test (N = 3 for each group). (F) The up-regulation of GFAP in *sacs*$^{-/-}$ retinas as detected by immunostaining. (G) Relative mRNA expression of inflammatory factors evaluated in *sacs*$^{-/-}$ larvae at 120 hpf. qRT-PCR analysis revealed an increase in the levels of inflammatory genes, normalized to *β-actin*. Three independent RNA samples from *sacs*$^{-/-}$ mutant larvae at 120 hpf and from controls. *$p < 0.05$, calculated by two-tailed Student's t-test. Error bars indicate mean ± s.e.m.

dying cells, Müller glia enter a proliferative state, migrate to the various cellular layers of the retina that have been damaged, and reveal their multipotential nature by differentiating into any type of retinal neuron (Nagashima and Hitchcock, 2021). For instance, after their death, photoreceptors release Tnfα, which is necessary and sufficient to reprogram Müller glia in the zebrafish retina (Iribarne et al., 2019). In our mutant study, we observed a marked increase of GFAP expression in *sacs*$^{-/-}$ retinas compared to controls (Fig. 8F) (Liu et al., 2022), indicating an activation of Müller glia cells. Real-time validation studies of inflammatory markers including *cox2*, *il-1b*, *cxcl8-l1*, and *tnfα* confirmed the presence of an inflammatory condition in *sacs*$^{-/-}$ retinas compared to controls (Fig. 8G).

4. Discussion

Beyond its major neurological manifestations, ARSACS can also impact visual function in patients (Tremblay et al., 2022), although the exact mechanisms behind retinal changes remain not fully understood. Distinctive retinal abnormalities may suggest retinal hyperplasia due to altered developmental patterns (Rezende Filho et al., 2021) such as thickening of RNFL. *Sacs* knock-out and knock-in mice exhibit early-onset ataxic, neurofilament bundling and early loss of Purkinje cells, followed later by the loss of spinal motor neurons, peripheral neuropathy, and muscle atrophy (Larivière et al., 2019; Larivière et al., 2015). However, visual defects have not been reported to date in in these models. Zebrafish are a key model for retinal biology due to their complex, cone-dominated visual system, similar to higher vertebrates. Their transparency allows real-time observation of retinal development, and their relatively large eyes facilitate early manipulation. The zebrafish retina rapidly grows and differentiates from hatching to around five days post-fertilization, reaching full development in terms of morphology, electrophysiology, and behavior (Morris and Fadool, 2005). In the *sacs*$^{-/-}$ zebrafish model (Naef et al., 2021), we observed a marked increase in the mitotic index, suggesting a potential delay or blockage in retinal neurogenesis. Disruptions in the cell cycle of retinal progenitor cells can lead to significant developmental changes in the retina. An abnormal increase in the mitotic rate of these progenitors often accompanies these disruptions, triggering a cascade of events that affect retinal layer formation and organization (Miles and Tropepe, 2016). This results in delayed differentiation, with fewer early-born retinal neurons and a higher proportion of later-developing cell types. Retinal differentiation begins at the center and extends toward the periphery as retinal progenitor cells (RPCs) develop into one of the five main types of retinal neurons—ganglion cells, horizontal cells, amacrine cells, bipolar cells, photoreceptor cells—and Müller glial cells, in that sequence (Miles and Tropepe, 2016). Consistent with this specific temporal sequence of retinal histogenesis and our hypothesis, *sacs*$^{-/-}$ larvae displayed a reduction in early-born RGCs along with an increase in later-born cell types such as amacrine cells, bipolar cells, and Müller glial cells. These cell cycle defects in retinal neuronal progenitors would typically be associated with an increase in eye size, rather than the moderate "microphthalmia" observed in 120 hpf mutants. This discrepancy was addressed through experimental observation, revealing a substantial increase in the apoptotic rate in *sacs*$^{-/-}$ developing retinas, primarily in the inner nuclear layer (INL), which is predominantly composed of later-generated neurons. Additionally, apoptotic cells were also noted (GCL) and (ONL) suggesting compromised survival of these cellular populations. This dual phenomenon could contribute to

structural abnormalities in the retinal layers (Linden et al., 1999; Pant et al., 2013). Consistently, we also found in mutant larvae structural disorganization in rod and cone photoreceptors and an increase in amacrine cells. From a more functional perspective, loss of sacsin reduced the navigational competence of larvae in a light environment, as well as their response to sudden bright light. This phenomenon suggests that progressive rod dysfunction leads to peripheral vision loss and photophobia (Noel et al., 2022). ERG analysis showed that the amplitude of the b-wave in *sacs* mutant animals is significantly larger at medium to bright light intensities. The b-wave reflects ON-pathway activation and can serve as a proxy for general excitability of the outer retina. Abnormal ERG has previously been reported in an ARSACS patient, but without detailed descriptions (Borruat et al., 2017). A possible contribution for the observed b-wave increase could reside in electric signal modulation exerted by amacrine cells, a cellular population that appears to be actually increased in *sacs* KO larvae. Amacrine innervation and tonic release of neurotransmitters and peptides on retinal second order neurons has a fundamental role in retinal physiology. Dopamine, for instance, is released by a group of distinctive amacrine cells, rising at dawn and following a circadian rhythm (Witkovsky, 2004) that has been observed to influence behavioral outcomes in light/dark conditions (Safarian et al., 2020). This suggests a possible function for dopamine to support cone-driven visual circuits, enhancing the photopic cone response by reducing negative feedback from horizontal cells (DeVries and Schwartz, 1989) and preparing the retina for photopic (daytime) vision (Witkovsky, 2004). Another possible contribution to ERG modification could come from electrical signals deriving from rod circuits. In spite of this, this hypothesis appear to be unlikely, as rod function does not significantly contribute to the larval zebrafish ERG before about 15 dpf (Noel et al., 2021), making it unlikely that changes in rod coupling underlie the enhanced ERG reported here. Alternatively, the increased responsiveness of bipolar cells observed here could result from the convergence of a reduced number of cone photoreceptors onto a normal number of second-order neurons. In this perspective, the photophobic freezing observed in mutant larvae could be a consequence of the combined dysplastic and degenerative phenotype stemming from the decline of the photoreceptor population. Notably, light hypersensitivity or glare are well-known and common symptomatic presentations in patients with Stargardt disease (Miedziak et al., 2000), Retinitis pigmentosa (Nguyen et al., 2023), Alström disease (Wang et al., 2022) and age-related macular degeneration (AMD). In the present study, molecular and behavioral analyses confirmed impaired visual function due to structural disorganization or loss of photoreceptors in *sacs*$^{-/-}$ retinas. Despite severe visual impairment and defects in retinal layering observed in mutant larvae, the neural-retinal identity appeared unaffected, with no observed transformation of the retina into pigmented cells. These findings imply that sacsin loss does not influence the early establishment or maintenance of neural retina identity. In our study, we also observed defects in axonal outgrowth, particularly in the optic tectum and the eye region, and about 1/3 of *sacs* mutant larvae showed structurally altered optic nerves. This could be a consequence of the slow progressive loss of RGCs. RGCs, due to their morphological features and high-energy requirements, are particularly vulnerable to mitochondrial dysfunction (Vernazza et al., 2021). Considering that the loss of sacsin presents a mitochondrial impairment and network disorganization (Bagaria et al., 2022; Girard et al., 2012; Morani et al., 2019), the mitochondrial deficits triggered by the loss of the sacsin could possibly result in inadequate energy supply in RGCs, contributing to cellular apoptosis observed in our mutants. Another important factor potentially contributing to retinal phenotypes observed in *sacs* KO zebrafish could reside in neuroinflammation. RNA-seq analysis in whole larvae showed an enrichment in genes involved in inflammation and oxidative stress response, key factors in the pathogenesis of many degenerative retinal diseases (Jadeja and Martin, 2021). In response to injury or disease, resident microglia to gather and release various growth factors and pro-inflammatory cytokines, stimulates Müller glia to regenerate lost neurons (Gao et al., 2021). Persistency of a chronic pro-inflammatory environment is a common denominator in retinal degenerative diseases, leading microglial cells to become pathologically activated and secrete excessive amounts of inflammatory mediators, thereby promoting tissue damage and exacerbating the disease (Rashid et al., 2019). Consistent with this hypothesis, together with photoreceptor loss in the dorsal retina we found in our model a) significant Müller activation, b) presence of reactive microglia with ameboid morphology and mostly localized in the GCL and outer retina, and c) an increase in mRNA expression of the inflammatory factors as *cox2b*, *il-1b*, *cxcl8-l1*, and *tnfα*. Loss of photoreceptors in mutant fish appears not only to be related to chronic intra-retinal inflammation, but also potentially to RPE dysfunction. In the zebrafish retina, the interaction between photoreceptors and adjacent RPE cells establishes a metabolic system crucial for maintaining overall vision health (Jaroszynska et al., 2021). In our model, We observed a significantly reduced thickness in the RPE of *sacs*$^{-/-}$ mutant retinas, together with imbalances in expression of fat-soluble vitamin-related proteins, such as ttpa (alpha-tocopherol transfer protein) and rdh5, respectively involved in vitamin E and A metabolism. In particular, vitamin E stands out as a powerful antioxidant, and is essential during embryonic development, especially in eye formation (Head et al., 2020). The RPE contains the highest concentrations of vitamin E, followed by the outer segments of photoreceptor cells (Edwards et al., 2022). One of the main functions of the RPE is the phagocytosis of shed photoreceptor outer segment disks, a process crucial for their proper recycling (Kwon and Freeman, 2020). Mutations in the *Ttpa* gene, coding for alpha-tocopherol transfer protein (α-TTP), lead to ataxia with deficiency of vitamin E, causing irreversible alterations to retinal structure and function (Edwards et al., 2022). In addition, several studies have shown that vitamin E deficiency can lead to macular degeneration due to increased oxidative stress and RPE metabolic dysfunction, resulting in focal disruption of the outer rod segments of photoreceptors (Gorusupudi et al., 2017), in a way that is reminiscent to what we observed in *sacs* KO mutant larvae. It is tempting to speculate the possible existence of an eye-specific depletion of vitamin E in ARSACS patients, and that vitamin E supplementation could possibly counteract retinal damage seen in *sacs* KO larvae. Another critical function of the RPE consists in chromophore regeneration in the visual cycle, which is strictly dependent on vitamin A levels. Modifications in vitamin A metabolism, as seen in *sacs* mutant larvae, could per se trigger mechanisms of retinal degeneration (reviewed in (Sajovic et al., 2022)). Finally, sacsin is a known chaperone protein, and could actually play a role in assisting the correct folding of opsins in photoreceptors, especially in rod outer segments where concentrations of this protein is maximal. Remarkably, misfolding and aggregation of opsins and other photoreceptor proteins is a well-known cause of retinal conditions as in Stargardt diseases (Tzekov et al., 2011)(Vasudevan et al., 2024).

5. Conclusions

In conclusion, we have successfully investigated the retinal degenerative phenotype in a *sacs* mutant zebrafish model. We demonstrated abnormal molecular signatures, altered visual-motor behavior, and cell cycle defects in progenitor cells. We can thus assume that loss of sacsin in zebrafish could be associated with a cone-rod dystrophy, leading to visual loss and light hypersensitivity. We acknowledge several limitations in our study, including the inherent differences between zebrafish and human retinal structures and developmental stages, which may affect the direct applicability of our results to patients. Further research is required to address these limitations. Nonetheless, the retinal phenotype observed in zebrafish mutants could mirror mild subclinical forms of retinal dystrophies seen in ARSACS patients, as supported by existing literature. Our model offers a valuable platform for understanding the long-term effects of sacsin depletion and for screening potential therapeutic options with immediate translational potential.

Supplementary data to this article can be found online at https://doi.

org/10.1016/j.nbd.2025.106793.

Funding

This work was supported in part by Fondazione Telethon (grants GSA21G006 and GSA24A001 to V.N.) and by Fondation de l'Ataxie Charlevoix-Saguenay (seed grant 2022 to V.N.). FMS is partially supported by the Italian Ministry of Health Grant RC25.

Ethics approval

This study does not include human samples. All animal procedures were authorized by the University of Pisa Animal Ethics Committee and the Italian Ministry of Health (approval number 338/2020-PR).

CRediT authorship contribution statement

Valentina Naef: Writing – review & editing, Writing – original draft, Visualization, Validation, Supervision, Resources, Project administration, Methodology, Investigation, Funding acquisition, Formal analysis, Data curation, Conceptualization. **Devid Damiani:** Writing – review & editing, Visualization, Methodology, Formal analysis, Data curation, Conceptualization. **Rosario Licitra:** Visualization, Methodology. **Maria Marchese:** Visualization, Methodology, Data curation. **Stefania Della Vecchia:** Visualization, Methodology. **Matteo Baggiani:** Visualization, Formal analysis. **Letizia Brogi:** Visualization, Methodology. **Daniele Galatolo:** Visualization, Methodology. **Silvia Landi:** Visualization, Software. **Filippo Maria Santorelli:** Writing – review & editing; Funding acquisition.

Declaration of competing interest

The authors declare that they have no conflicts of interest.

Data availability

Data will be made available on request.

Acknowledgements

We are grateful to Dr. Baldassare Fronte of the University of Pisa for his technical support in the management of the zebrafish facility. We thank Prof. Francesca Abramo for her technical support on histological analysis. The authors thank the Italian patients' association (ARSACS OdV) and the ARSACS Foundation for their constant encouragement and support.

References

Aly, K.A., Moutaoufik, M.T., Zilocchi, M., Phanse, S., Babu, M., 2022. Insights into SACS pathological attributes in autosomal recessive spastic ataxia of Charlevoix-Saguenay (ARSACS)☆. Curr. Opin. Chem. Biol. 71, 102211. https://doi.org/10.1016/j.cbpa.2022.102211.

Angueyra, J.M., Kindt, K.S., 2018. Leveraging zebrafish to study retinal degenerations. Front. Cell Dev. Biol. 6, 110. https://doi.org/10.3389/fcell.2018.00110.

Appell, M.B., Pejavar, J., Pasupathy, A., Rompicharla, S.V.K., Abbasi, S., Malmberg, K., Kolodziejski, P., Ensign, L.M., 2024. Next generation therapeutics for retinal neurodegenerative diseases. J. Control. Release 367, 708–736. https://doi.org/10.1016/j.jconrel.2024.01.063.

Bagaria, J., Bagyinszky, E., An, S.S.A., 2022. Genetics of autosomal recessive spastic Ataxia of Charlevoix-Saguenay (ARSACS) and role of Sacsin in neurodegeneration. Int. J. Mol. Sci. 23. https://doi.org/10.3390/ijms23010552.

Borruat, F.-X., Holder, G.E., Bremner, F., 2017. Inner retinal dysfunction in the autosomal recessive spastic Ataxia of Charlevoix-Saguenay. Front. Neurol. 8. https://doi.org/10.3389/fneur.2017.00523.

Bouhlal, Y., Amouri, R., El Euch-Fayeche, G., Hentati, F., 2011. Autosomal recessive spastic ataxia of Charlevoix-Saguenay: an overview. Parkinsonism Relat. Disord. 17, 418–422. https://doi.org/10.1016/j.parkreldis.2011.03.005.

Bracher, M., Madi-Segwagwe, B.C., Winstanley, E., Gillan, H., Long-Sutehall, T., 2021. Family refusal of eye tissue donation from potential solid organ donors: a retrospective analysis of summary and free-text data from the UK National Health Service Blood and transplant services (NHS-BT) National Referral Centre (1 April 2014 to 31 March 2). BMJ Open 11, e045250. https://doi.org/10.1136/bmjopen-2020-045250.

Brogi, L., Marchese, M., Cellerino, A., Licitra, R., Naef, V., Mero, S., Bibbiani, C., Fronte, B., 2021. β-Glucans as dietary supplement to improve locomotion and mitochondrial respiration in a model of Duchenne muscular dystrophy. Nutrients 13, 1619. https://doi.org/10.3390/nu13051619.

Burton, C.E., Zhou, Y., Bai, Q., Burton, E.A., 2017. Spectral properties of the zebrafish visual motor response. Neurosci. Lett. 646, 62–67. https://doi.org/10.1016/j.neulet.2017.03.002.

Camussi, D., Naef, V., Brogi, L., Della Vecchia, S., Marchese, M., Nicoletti, F., Santorelli, F.M., Licitra, R., 2024. Delving into the complexity of valproate-induced autism Spectrum disorder: the use of zebrafish models. Cells 13, 1349. https://doi.org/10.3390/cells13161349.

Chen, J., Lei, L., Tian, L., Hou, F., Roper, C., Ge, X., Zhao, Y., Chen, Y., Dong, Q., Tanguay, R.L., Huang, C., 2018. Developmental and behavioral alterations in zebrafish embryonically exposed to valproic acid (VPA): An aquatic model for autism. Neurotoxicol. Teratol. 66, 8–16. https://doi.org/10.1016/j.ntt.2018.01.002.

Davison, J.E., 2020. Eye involvement in inherited metabolic disorders. Ther. Adv. Ophthalmol. 12, 251584142097910. https://doi.org/10.1177/2515841420979109.

Della Vecchia, S., Ogi, A., Licitra, R., Abramo, F., Nardi, G., Mero, S., Landi, S., Battini, R., Sicca, F., Ratto, G.M., Santorelli, F.M., Marchese, M., 2022. Trehalose treatment in zebrafish model of Lafora disease. Int. J. Mol. Sci. 23, 6874. https://doi.org/10.3390/ijms23126874.

DeVries, S.H., Schwartz, E.A., 1989. Modulation of an electrical synapse between solitary pairs of catfish horizontal cells by dopamine and second messengers. J. Physiol. 414, 351–375. https://doi.org/10.1113/jphysiol.1989.sp017692.

Edwards, G., Olson, C.G., Euritt, C.P., Koulen, P., 2022. Molecular mechanisms underlying the therapeutic role of vitamin E in age-related macular degeneration. Front. Neurosci. 16. https://doi.org/10.3389/fnins.2022.890021.

Gao, H.A.L., Huang, X., Chen, X., Xu, H., 2021. Müller glia-mediated retinal regeneration. Mol. Neurobiol. 58, 2342–2361. https://doi.org/10.1007/s12035-020-02274-w.

Girard, M., Larivière, R., Parfitt, D.A., Deane, E.C., Gaudet, R., Nossova, N., Blondeau, F., Prenosil, G., Vermeulen, E.G.M., Duchen, M.R., Richter, A., Shoubridge, E.A., Gehring, K., McKinney, R.A., Brais, B., Chapple, J.P., McPherson, P.S., 2012. Mitochondrial dysfunction and Purkinje cell loss in autosomal recessive spastic ataxia of Charlevoix-Saguenay (ARSACS). Proc. Natl. Acad. Sci. 109, 1661–1666. https://doi.org/10.1073/pnas.1113166109.

Gorusupudi, A., Nelson, K., Bernstein, P.S., 2017. The age-related eye disease 2 study: micronutrients in the treatment of macular degeneration. Adv. Nutr. 8, 40–53. https://doi.org/10.3945/an.116.013177.

Guo, L., Choi, S., Bikkannavar, P., Cordeiro, M.F., 2022. Microglia: key players in retinal ageing and neurodegeneration. Front. Cell. Neurosci. 16, 804782. https://doi.org/10.3389/fncel.2022.804782.

Head, B., La Du, J., Tanguay, R.L., Kioussi, C., Traber, M.G., 2020. Vitamin E is necessary for zebrafish nervous system development. Sci. Rep. 10, 15028. https://doi.org/10.1038/s41598-020-71760-x.

Iribarne, M., Hyde, D.R., 2022. Different inflammation responses modulate Müller glia proliferation in the acute or chronically damaged zebrafish retina. Front. Cell Dev. Biol. 10. https://doi.org/10.3389/fcell.2022.892271.

Iribarne, M., Hyde, D.R., Masai, I., 2019. TNFα induces Müller glia to transition from non-proliferative gliosis to a regenerative response in mutant zebrafish presenting chronic photoreceptor degeneration. Front. Cell Dev. Biol. 7, 296. https://doi.org/10.3389/fcell.2019.00296.

Jadeja, R.N., Martin, P.M., 2021. Oxidative stress and inflammation in retinal degeneration. Antioxidants 10, 790. https://doi.org/10.3390/antiox10050790.

Jaroszynska, N., Harding, P., Moosajee, M., 2021. Metabolism in the zebrafish retina. J. Dev. Biol. 9, 10. https://doi.org/10.3390/jdb9010010.

Koke, J.R., Mosier, A.L., García, D.M., 2010. Intermediate filaments of zebrafish retinal and optic nerve astrocytes and Müller glia: differential distribution of cytokeratin and GFAP. BMC. Res. Notes 3, 50. https://doi.org/10.1186/1756-0500-3-50.

Kwon, W., Freeman, S.A., 2020. Phagocytosis by the retinal pigment epithelium: recognition, resolution. Recycling. Front. Immunol. 11. https://doi.org/10.3389/fimmu.2020.604205.

Larivière, R., Gaudet, R., Gentil, B.J., Girard, M., Conte, T.C., Minotti, S., Leclerc-Desaulniers, K., Gehring, K., McKinney, R.A., Shoubridge, E.A., McPherson, P.S., Durham, H.D., Brais, B., 2015. Sacs knockout mice present pathophysiological defects underlying autosomal recessive spastic ataxia of Charlevoix-Saguenay. Hum. Mol. Genet. 24, 727–739. https://doi.org/10.1093/hmg/ddu491.

Larivière, R., Sgarioto, N., Márquez, B.T., Gaudet, R., Choquet, K., McKinney, R.A., Watt, A.J., Brais, B., 2019. Sacs R272C missense homozygous mice develop an ataxia phenotype. Mol. Brain 12, 19. https://doi.org/10.1186/s13041-019-0438-3.

Le, H.-G.T., Dowling, J.E., Cameron, D.J., 2012. Early retinoic acid deprivation in developing zebrafish results in microphthalmia. Vis. Neurosci. 29, 219–228. https://doi.org/10.1017/S0952523812000296.

Letelier, J., Buono, L., Almuedo-Castillo, M., Zang, J., Mounieres, C., González-Díaz, S., Polvillo, R., Sanabria-Reinoso, E., Corbacho, J., Sousa-Ortega, A., Diez del Corral, R., Neuhauss, S.C., Martínez-Morales, J.R., 2023. Mutation of vsx genes in zebrafish highlights the robustness of the retinal specification network. Elife 12. https://doi.org/10.7554/eLife.85594.

Linden, R., Rehen, S.K., Chiarini, L.B., 1999. Apoptosis in developing retinal tissue. Prog. Retin. Eye Res. 18, 133–165. https://doi.org/10.1016/S1350-9462(98)00020-2.

Liu, F., Qin, Y., Huang, Y., Gao, P., Li, J., Yu, S., Jia, D., Chen, X., Lv, Y., Tu, J., Sun, K., Han, Y., Reilly, J., Shu, X., Lu, Q., Tang, Z., Xu, C., Luo, D., Liu, M., 2022. Rod genesis driven by mafba in an nrl knockout zebrafish model with altered

photoreceptor composition and progressive retinal degeneration. PLoS Genet. 18, e1009841. https://doi.org/10.1371/journal.pgen.1009841.
MacArthur Clark, J., 2018. The 3Rs in research: a contemporary approach to replacement, reduction and refinement. Br. J. Nutr. 120, S1–S7. https://doi.org/10.1017/S0007114517002227.
Marchese, M., Bernardi, S., Ogi, A., Licitra, R., Silvi, G., Mero, S., Galatolo, D., Gammaldi, N., Doccini, S., Ratto, G.M., Rapposelli, S., Neuhauss, S.C.F., Zang, J., Rocchiccioli, S., Michelucci, E., Ceccherini, E., Santorelli, F.M., 2024. Targeting autophagy impairment improves the phenotype of a novel CLN8 zebrafish model. Neurobiol. Dis. 197, 106536. https://doi.org/10.1016/j.nbd.2024.106536.
Masek, M., Zang, J., Mateos, J.M., Garbelli, M., Ziegler, U., Neuhauss, S.C.F., Bachmann-Gagescu, R., 2023. Studying the morphology, composition and function of the photoreceptor primary cilium in zebrafish. Methods Cell Biol. 97–128. https://doi.org/10.1016/bs.mcb.2022.10.004.
Maurer, C.M., Schönthaler, H.B., Mueller, K.P., Neuhauss, S.C.F., 2010. Distinct retinal deficits in a zebrafish pyruvate dehydrogenase-deficient mutant. J. Neurosci. 30, 11962–11972. https://doi.org/10.1523/JNEUROSCI.2848-10.2010.
Mero, S., Salviati, L., Leuzzi, V., Rubegni, A., Calderan, C., Nardecchia, F., Galatolo, D., Desbats, M.A., Naef, V., Gemignani, F., Novelli, M., Tessa, A., Battini, R., Santorelli, F.M., Marchese, M., 2021. New pathogenic variants in COQ4 cause ataxia and neurodevelopmental disorder without detectable CoQ10 deficiency in muscle or skin fibroblasts. J. Neurol. https://doi.org/10.1007/s00415-021-10509-6.
Miedziak, A.I., Perski, T., Andrews, P.P., Donoso, L.A., 2000. Stargardt's macular dystrophy–a patient's perspective. Optometry 71, 165–176.
Miles, A., Tropepe, V., 2016. Coordinating progenitor cell cycle exit and differentiation in the developing vertebrate retina. Neurogenesis 3, e1161697. https://doi.org/10.1080/23262133.2016.1161697.
Mitchell, D.M., Lovel, A.G., Stenkamp, D.L., 2018. Dynamic changes in microglial and macrophage characteristics during degeneration and regeneration of the zebrafish retina. J. Neuroinflammation 15, 163. https://doi.org/10.1186/s12974-018-1185-6.
Morani, F., Doccini, S., Sirica, R., Paterno, M., Pezzini, F., Ricca, I., Simonati, A., Delledonne, M., Santorelli, F.M., 2019. Functional transcriptome analysis in ARSACS KO cell model reveals a role of Sacsin in autophagy. Sci. Rep. 9, 11878. https://doi.org/10.1038/s41598-019-48047-x.
Morris, A.C., Fadool, J.M., 2005. Studying rod photoreceptor development in zebrafish. Physiol. Behav. 86, 306–313. https://doi.org/10.1016/j.physbeh.2005.08.020.
Naef, V., Marchese, M., Ogi, A., Fichi, G., Galatolo, D., Licitra, R., Doccini, S., Verri, T., Argenton, F., Morani, F., Santorelli, F.M., 2021. Efficient neuroprotective rescue of sacsin-related disease Phenotypes in zebrafish. Int. J. Mol. Sci. 22, 8401. https://doi.org/10.3390/ijms22168401.
Nagashima, M., Hitchcock, P.F., 2021. Inflammation regulates the multi-step process of retinal regeneration in zebrafish. Cells 10, 783. https://doi.org/10.3390/cells10040783.
Nguyen, X.-T.-A., Moekotte, L., Plomp, A.S., Bergen, A.A., van Genderen, M.M., Boon, C. J.F., 2023. Retinitis Pigmentosa: current clinical management and emerging therapies. Int. J. Mol. Sci. 24. https://doi.org/10.3390/ijms24087481.
Niklaus, S., Kirla, K.T., Kraemer, T., Groh, K., Schirmer, K., Neuhauss, S., 2017. Cocaine accumulation in zebrafish eyes leads to augmented amplitudes in the Electroretinogram. Matters. https://doi.org/10.19185/matters.201703000003.
Noel, N.C.L., MacDonald, I.M., Allison, W.T., 2021. Zebrafish models of photoreceptor dysfunction and degeneration. Biomolecules 11, 78. https://doi.org/10.3390/biom11010078.
Noel, N.C.L., Allison, W.T., MacDonald, I.M., Hocking, J.C., 2022. Zebrafish and inherited photoreceptor disease: models and insights. Prog. Retin. Eye Res. 91, 101096. https://doi.org/10.1016/j.preteyeres.2022.101096.
Olufunmilayo, E.O., Gerke-Duncan, M.B., Holsinger, R.M.D., 2023. Oxidative stress and antioxidants in neurodegenerative disorders. Antioxidants 12, 517. https://doi.org/10.3390/antiox12020517.
Pant, S.D., March, L.D., Famulski, J.K., French, C.R., Lehmann, O.J., Waskiewicz, A.J., 2013. Molecular mechanisms regulating ocular apoptosis in zebrafish gdf6a mutants. Investig. Opthalmol. Vis. Sci. 54, 5871. https://doi.org/10.1167/iovs.12-11315.
Parkinson, M.H., Bartmann, A.P., Clayton, L.M.S., Nethisinghe, S., Pfundt, R., Chapple, J. P., Reilly, M.M., Manji, H., Wood, N.J., Bremner, F., Giunti, P., 2018. Optical coherence tomography in autosomal recessive spastic ataxia of Charlevoix-Saguenay. Brain 141, 989–999. https://doi.org/10.1093/brain/awy028.
Rashid, K., Akhtar-Schaefer, I., Langmann, T., 2019. Microglia in retinal degeneration. Front. Immunol. 10. https://doi.org/10.3389/fimmu.2019.01975.
Rezende Filho, F.M., Bremner, F., Pedroso, J.L., de Andrade, J.B.C., Marianelli, B.F., Lourenço, C.M., Marques-Júnior, W., França, M.C., Kok, F., Sallum, J.M.F., Parkinson, M.H., Barsottini, O.G., Giunti, P., 2021. Retinal architecture in autosomal recessive spastic Ataxia of Charlevoix-Saguenay (ARSACS): insights into disease pathogenesis and biomarkers. Mov. Disord. 36, 2027–2035. https://doi.org/10.1002/mds.28612.
Rock, S., Rodenburg, F., Schaaf, M.J.M., Tudorache, C., 2022. Detailed analysis of zebrafish larval behaviour in the light dark challenge assay shows that diel hatching time determines individual variation. Front. Physiol. 13. https://doi.org/10.3389/fphys.2022.827282.
Rodwell, V., Patil, M., Kuht, H.J., Neuhauss, S.C.F., Norton, W.H.J., Thomas, M.G., 2023. Zebrafish optokinetic reflex: minimal reporting guidelines and recommendations. Biology (Basel). 13. https://doi.org/10.3390/biology13010004.
Romano, A., Tessa, A., Barca, A., Fattori, F., Fulvia de Leva, M., Terracciano, A., Storelli, C., Santorelli, F.M., Verri, T., 2013. Comparative analysis and functional mapping of SACS mutations reveal novel insights into Sacsin repeated architecture. Hum. Mutat. 34, 525–537. https://doi.org/10.1002/humu.22269.
Rovira, M., Miserocchi, M., Montanari, A., Hammou, L., Chomette, L., Pozo, J., Imbault, V., Bisteau, X., Wittamer, V., 2023. Zebrafish galectin 3 binding protein is the target antigen of the microglial 4C4 monoclonal antibody. Dev. Dyn. 252, 400–414. https://doi.org/10.1002/dvdy.549.
Sabaliauskas, N.A., Foutz, C.A., Mest, J.R., Budgeon, L.R., Sidor, A.T., Gershenson, J.A., Joshi, S.B., Cheng, K.C., 2006. High-throughput zebrafish histology. Methods 39, 246–254. https://doi.org/10.1016/j.ymeth.2006.03.001.
Safarian, N., Whyte-Fagundes, P., Zoidl, C., Grigull, J., Zoidl, G., 2020. Visuomotor deficiency in panx1a knockout zebrafish is linked to dopaminergic signaling. Sci. Rep. 10, 9538. https://doi.org/10.1038/s41598-020-66378-y.
Sahu, B., Maeda, A., 2016. Retinol dehydrogenases regulate vitamin a metabolism for visual function. Nutrients 8, 746. https://doi.org/10.3390/nu8110746.
Sajovic, J., Meglič, A., Glavač, D., Markelj, Š., Hawlina, M., Fakin, A., 2022. The role of vitamin a in retinal diseases. Int. J. Mol. Sci. 23. https://doi.org/10.3390/ijms23031014.
Shao, F., Wang, X., Wu, H., Wu, Q., Zhang, J., 2022. Microglia and Neuroinflammation: crucial pathological mechanisms in traumatic brain injury-induced neurodegeneration. Front. Aging Neurosci. 14, 825086. https://doi.org/10.3389/fnagi.2022.825086.
Steenbergen, P.J., Richardson, M.K., Champagne, D.L., 2011. Patterns of avoidance behaviours in the light/dark preference test in young juvenile zebrafish: a pharmacological study. Behav. Brain Res. 222, 15–25. https://doi.org/10.1016/j.bbr.2011.03.025.
Takiyama, Y., 2006. Autosomal recessive spastic ataxia of Charlevoix-Saguenay. Neuropathology 26, 368–375. https://doi.org/10.1111/j.1440-1789.2006.00664.x.
Takiyama, Y., 2007. Sacsinopathies: Sacsin-related ataxia. Cerebellum 6, 353–359. https://doi.org/10.1080/14734220701230466.
Tremblay, M., Girard-Côté, L., Brais, B., Gagnon, C., 2022. Documenting manifestations and impacts of autosomal recessive spastic ataxia of Charlevoix–Saguenay to develop patient-reported outcome. Orphanet J. Rare Dis. 17, 369. https://doi.org/10.1186/s13023-022-02497-1.
Tzekov, R., Stein, L., Kaushal, S., 2011. Protein misfolding and retinal degeneration. Cold Spring Harb. Perspect. Biol. 3, a007492. https://doi.org/10.1101/cshperspect.a007492.
Vasudevan, S., Senapati, S., Pendergast, M., Park, P.S.-H., 2024. Aggregation of rhodopsin mutants in mouse models of autosomal dominant retinitis pigmentosa. Nat. Commun. 15, 1451. https://doi.org/10.1038/s41467-024-45748-4.
Venkatraman, P., Mills-Henry, I., Padmanabhan, K.R., Pascuzzi, P., Hassan, M., Zhang, J., Zhang, X., Ma, P., Pang, C.P., Dowling, J.E., Zhang, M., Leung, Y.F., 2020. Rods contribute to visual behavior in larval zebrafish. Investig. Opthalmol. Vis. Sci. 61, 11. https://doi.org/10.1167/iovs.61.12.11.
Vermeer, S., van de Warrenburg, B.P., Kamsteeg, E.-J., Brais, B., Synofzik, M., 1993. ARSACS, GeneReviews®.
Vernazza, S., Oddone, F., Tirendi, S., Bassi, A.M., 2021. Risk factors for retinal ganglion cell distress in Glaucoma and neuroprotective potential intervention. Int. J. Mol. Sci. 22, 7994. https://doi.org/10.3390/ijms22157994.
Wan, J., Goldman, D., 2016. Retina regeneration in zebrafish. Curr. Opin. Genet. Dev. 40, 41–47. https://doi.org/10.1016/j.gde.2016.05.009.
Wang, Y., Huang, L., Sun, L., Li, S., Zhang, Z., Zhang, T., Lai, Y., Ding, X., 2022. Ocular findings and genetic test in Alström syndrome in childhood. Exp. Eye Res. 225, 109277. https://doi.org/10.1016/j.exer.2022.109277.
Witkovsky, P., 2004. Dopamine and retinal function. Doc. Ophthalmol. 108, 17–39. https://doi.org/10.1023/B:DOOP.0000019487.88486.0a.
Yu-Wai-Man, P., Pyle, A., Griffin, H., Santibanez-Korev, M., Horvath, R., Chinnery, P.F., 2014. Abnormal retinal thickening is a common feature among patients with ARSACS-related phenotypes: table 1. Br. J. Ophthalmol. 98, 711–713. https://doi.org/10.1136/bjophthalmol-2013-304534.
Zang, J., Neuhauss, S.C.F., 2021. Biochemistry and physiology of zebrafish photoreceptors. Pflügers Arch. - Eur. J. Physiol. 473, 1569–1585. https://doi.org/10.1007/s00424-021-02528-z.
Zhong, J.-X., Zhou, L., Li, Z., Wang, Y., Gui, J.-F., 2014. Zebrafish Noxa promotes mitosis in early embryonic development and regulates apoptosis in subsequent embryogenesis. Cell Death Differ. 21, 1013–1024. https://doi.org/10.1038/cdd.2014.22.